Soil Biology & Biochemistry 50 (2012) 118–125

Contents lists available at SciVerse ScienceDirect

Soil Biology & Biochemistry

journal homepage: www.elsevier.com/locate/soilbio

Linkages between soil micro-site properties and CO_2 and N_2O emissions during a simulated thaw for a northern prairie Mollisol☆

Abbey F. Wick [a,*], Rebecca L. Phillips [b], Mark A. Liebig [b], Mark West [c], W. Lee Daniels [a]

[a] Virginia Tech, Department of Crop and Soil Environmental Sciences, Blacksburg, VA 24061-0404, USA
[b] United States Department of Agriculture, Agricultural Research Service, Northern Great Plains Research Laboratory, 1701 10th Avenue SW, Mandan, ND 58554, USA
[c] United States Department of Agriculture, Agricultural Research Service, Fort Collins, CO, 80526, USA

ARTICLE INFO

Article history:
Received 27 October 2011
Received in revised form
17 January 2012
Accepted 12 March 2012
Available online 27 March 2012

Keywords:
Global warming
Greenhouse gases
Nitrogen
Particulate organic matter

ABSTRACT

Biologically derived emissions of carbon dioxide (CO_2) and nitrous oxide (N_2O) at 0 °C vary with soil depth during soil thawing. Micro-site soil properties, especially those which influence porosity and substrate availability, also vary with depth and may help explain gas emissions. Intact soil cores collected to a depth of 80 cm from an undisturbed prairie Mollisol in central North Dakota were uniformly subjected to distinct temperature steps during a simulated soil thaw (−15 to 5 °C) and sampled for CO_2 and N_2O emissions throughout the soil profile. Emission data were fit to a first order exponential equation ($E = \alpha e^{\beta T}$). Cores were then analyzed in 10 cm depth increments for micro-site properties including root length and mass, aggregation, and organic substrate availability (available, aggregate-protected and mineral-bound pools). Both CO_2 and N_2O emissions at 0 °C declined exponentially with depth. Emissions of CO_2 and N_2O at 0 °C were strongly related to root length ($R^2 = 0.80$ and 0.76, respectively), root mass ($R^2 = 0.56$ and 0.74), large macroaggregate mass ($R^2 = 0.63$ and 0.54), and aggregate-protected organic matter ($R^2 > 0.57$), while available organic matter was related to CO_2 ($R^2 > 0.60$) and not N_2O. When CO_2 and N_2O emissions were normalized by available and aggregate-protected carbon pools, respectively, nutrient use efficiency increased significantly with depth. Results suggest CO_2 and N_2O emissions are (1) positively influenced by the rhizosphere and (2) differentially affected by substrate pool or location. CO_2 emissions were more positively affected by available substrate, while N_2O emissions were more positively affected by less labile, aggregate-protected substrate.

1. Introduction

Emissions of carbon dioxide (CO_2) and nitrous oxide (N_2O) vary between surface and subsurface soils during thawing (Fierer et al., 2003a, 2005; Davidson et al., 2006; Risk et al., 2008). These differences in emissions with depth have been attributed to environmentally-driven parameters such as temperature buffering (Burton and Beauchamp, 1994; van Bochove et al., 2000a) and moisture distributions (Fierer et al., 2003a; del Prado et al., 2006) throughout the soil profile. Other studies have also identified important soil properties or processes related to trace gas emissions, such as porosity (Phillips et al., 2012), microbial functional group stratification (Fierer et al., 2003b), rhizosphere priming (Zhu and Cheng, 2011), and variability in carbon (C) and nitrogen (N) content (Risk et al., 2008). When the environmental variables of temperature and moisture are similar at multiple soil depths, substrate availability is considered a fundamental driver to biogenic gas emissions from soils during thawing (Paul and Clark, 1996; Sehy et al., 2004). Substrate availability varies throughout the soil profile, subsequently influencing CO_2 and N_2O gas production from surface and subsurface sources.

Near the soil surface, high-quality organic substrates (root detritus and exudates as well as recent plant litter inputs) are relatively abundant, while subsoil material is generally lower in organic substrate quality and quantity (Ajwa et al., 1998; Jobbágy and Jackson, 2000; Fierer et al., 2003a,b; Fang et al., 2005). Stratification of organic substrate across depths contributes to the creation of soil micro-sites (defined as environments or locations where biological processes differ from those occurring in the whole soil; Gregorich et al., 2001), which are considered to be potential "hot spots" for CO_2 and N_2O production (Parkin, 1987; Sexstone et al., 1988; Sey et al., 2008). Micro-sites become increasingly important

☆ Mention of trade names or commercial products in this publication is solely for the purpose of providing specific information and does not imply recommendation or endorsement by the U.S. Department of Agriculture. USDA is an equal opportunity provider and employer.

* Corresponding author. Tel.: +1 540 231 0793; fax: +1 540 231 7630.
E-mail address: afwick@vt.edu (A.F. Wick).

0038-0717/$ – see front matter © 2012 Elsevier Ltd. All rights reserved.
doi:10.1016/j.soilbio.2012.03.010

for gas emissions during thawing in highly aggregated soils, where physical soil attributes (i.e. aggregation) influence root penetration patterns into soil (Bronick and Lal, 2005) and drive substrate availability (Christensen and Christensen, 1991; van Bochove et al., 2000a,b; Plante et al., 2009). During freeze-thaw events, micro-sites (substrate locality) play a larger role because substrate liberated by freezing is available immediately for use by microorganisms *in situ* (Sehy et al., 2004).

Micro-site characteristics arise primarily from rooting patterns, aggregation, substrate quality and distribution in soils (van Bochove et al., 2000b; Davidson and Janssens, 2006; Sey et al., 2008). Rooting patterns influence micro-sites by providing organic substrate for microbial communities and facilitating aggregate formation from individual soil particles (Killham, 1994; Paul and Clark, 1996; Bronick and Lal, 2005). Aggregation contributes to variability in pore size distributions important for gas transfer throughout the soil (Hillel, 1982) as well as to the compartmentalization or locality of organic substrates where decomposers are physically isolated from soil substrates (Plante et al., 2009). The total amount of measured substrate collected from the whole soil may be distributed disproportionately among pools located inside aggregates (aggregate-protected), on the outside of aggregates (available), or bound to soil minerals (mineral-bound; Paul and Clark, 1996; Six et al., 1998). All three substrate pools (both quality and quantity) are unique as a result of their spatial distribution throughout the soil. For example, organic matter in the available pool tends to be a higher quality substrate than aggregate-protected organic matter, which is subsequently of higher quality than mineral-bound organic matter (Jastrow and Miller, 1998). Though the available pool is the highest quality, it is also the smallest of the three pools, with the mineral-bound pool being the largest (Carter, 1996). The quality and quantity of these three pools likely varies with depth as root and aggregate properties shift within the soil profile, particularly between the surface and subsoil.

Micro-site properties are often not preserved during field sampling, limiting our understanding of how these properties might influence CO_2 and N_2O emissions (Silver et al., 2005; Risk et al., 2008; Phillips et al., 2012) especially when attempts are made to hold the environmental parameters of temperature and moisture constant throughout the soil profile (which can only be done in lab experiments). To identify potential micro-site controls on CO_2 and N_2O emissions with depth, we exposed intact prairie Mollisol cores (including both the surface soil and subsoil) to a simulated soil thaw (where all depths were exposed to the same temperature steps) while preserving structure and maintaining constant soil moisture across all depths. Data fit to a first order exponential equation ($E = \alpha e^{\beta T}$; van't Hoff, 1898) indicated emissions at 0 °C (α) varied with depth while microbial temperature responses ($Q_{10} = e^{\beta \times 10}$) to thawing were similar with depth (Phillips et al., 2012). We investigated these particular soils further to determine if micro-site soil properties (root mass and length, aggregation and soil organic matter pools) contribute to variation in emissions with depth of CO_2 and N_2O at 0 °C for a highly aggregated, undisturbed prairie Mollisol.

2. Materials and methods

2.1. Site information and field sampling

A historically-native grassland enclosure (23 ha) with no history of tillage was selected at the USDA-ARS Northern Great Plains Research Laboratory (NGPRL) in south-central North Dakota (46°46′N, 100°55′W). The site is managed for annual hay production and has not been grazed by cattle or fertilized for over 11 years. Soils are Temvik-Wilton silt loams (FAO: Calcic Siltic Chernozems; USDA: Fine-silty, mixed, superactive, frigid Typic and Pachic Haplustolls; Soil Survey Staff, 2010). Climate is semiarid with mean annual temperature of 5 °C and mean annual precipitation of 41.2 cm. Soil samples were collected from the southwest corner of the enclosure where vegetation was dominated by *Schizachyrium scoparium* (Michx.) Nash in October 2009. Soil cores were collected along a 30-m, north–south transect from six points spaced approximately 5 m apart. At each point, a pair of intact cores (located <0.3 m from each other) was collected using a hydraulic tractor press (Giddings Machine Co., Inc, Windsor, CO) with a plastic sleeve insert (7.65 cm dia. × 90 cm length) to avoid compaction of the cores during collection. Water filled pore space was 55% throughout the entire soil core at time of sample collection (Phillips et al., 2012).

All six pairs of cores were exposed to simulated thaw incubations, with pairs one through five used for gas and soil analyses and the sixth pair of cores used to track soil temperature (using a Omega Model HH21, Type *E* temperature sensor inserted in the 50–80 cm section of the core) and non-biogenic core emissions (autoclaved; Phillips et al., 2012) during the incubation. The first set of five cores was designated for measurement of biogenic emissions of CO_2 and N_2O using multiple 5 °C temperature-step incubations followed by analyses for general physiochemical soil properties (pH, nitrate-N, ammonium-N, total phosphorous, whole soil C and N, texture, bulk density, water filled pore space and porosity; Phillips et al., 2012). The second set of five cores was reserved for analysis of micro-site properties (roots, aggregation and organic matter pools) post-incubation.

For full details on the measurement and modeling of CO_2 and N_2O emissions with depth during temperature-step incubations and relations with whole soil properties see Phillips et al. (2012). Briefly, the cores reserved for gas measurements were transferred into incubation chambers constructed with polyvinyl chloride (PVC) tubes with sampling port locations at 15, 30, 45, 60 and 75 cm soil depths. Small soil cores at port locations were removed and perforated Bev-Line® tubing was inserted and secured with a threaded brass fitting and septum creating an airtight connection for gas sampling at port locations. The cores were placed in a Queue Cryostar Model 7110 (Queue Systems, Parkersburg, WV) freezer instrumented with T107 temperature sensors that logged one-minute temperature data with a 21X datalogger (Campbell Scientific, Logan, UT). All cores were gradually (0.5 °C h^{-1}) brought to −15 °C, which was sustained for 48 h. All cores were then uniformly subjected to sequential, 5 °C temperature-step incubations (−15 to −10 °C, −10 to −5 °C, −5 to 0 °C, and 0 to 5 °C), according to temperature probe data collected within the dedicated soil core (Phillips et al., 2012). These temperatures are commonly observed in soils in the northern prairie, so we exposed all soil depths to these specific temperature ranges to determine the temperature dependence of CO_2 and N_2O with depth. Each temperature step (i.e. −15 to −10 °C) occurred over a 7 h time period with temperature increasing at a rate of 0.5 °C h^{-1} and a stabilization period at each temperature of 2 h prior to sampling. We aimed to minimize methodological weakness by collecting soils just prior to freezing and controlling temperature with mesocosms (Henry, 2007). Post-sampling, ports were flushed with ultrapure N_2 and vented (fittings removed from all ports) for 12 h at each temperature step. Gas samples were analyzed using a Varian Model 3800 Gas Chromatograph with Combi-Pal autosampler. Incubations were completed within 28 d of core collection to minimize potential changes to microbial communities in the laboratory (Gödde and Conrad, 1999; Mikan et al., 2002).

Gas concentrations were converted to emissions using the bulk density of the soils immediately surrounding each gas port for the 460 cm^3 of soil (46 cm^2 area × 10 cm depth). We used the same volume for each gas sampling depth. The use of intact soil cores precluded the quantification of specific areas for each gas sampling depth. However, we minimized this effect by incubating long

enough to observe a measurable difference in gas production while minimizing the time for diffusive transport out of our defined zones (see Phillips et al., 2012 for more detail).

Measured CO_2 and N_2O emissions were then fit to a simple, first-order exponential equation [$E = \alpha e^{\beta T}$; where E is emission of CO_2 or N_2O (nmol CO_2 or pmol N_2O g^{-1} h^{-1}), T is the measured soil temperature (°C), and α (emission of CO_2 or N_2O when $T = 0$ °C) and β (units = 1/°C) are fitted parameters; van't Hoff, 1898]. Though CO_2 and N_2O temperature responses did not vary with depth, emissions of CO_2 and N_2O at 0 °C were found to exponentially decrease with depth suggesting dependence of emissions on soil micro-site properties as they shift throughout the soil profile (Phillips et al., 2012). While actual N_2O emissions data are typically not normally distributed, CO_2 and N_2O emissions at 0 °C were normally distributed and subsequently analyzed.

2.2. Physiochemical soil property analyses

Prior to micro-site soil analyses, a morphological description of a representative core was conducted according to Natural Resources Conservation Service (NRCS) protocol (Table 1). Briefly, the mollic epipedon was observed to a depth of 36 cm and underlain by combined sequence of Bw horizons with angular blocky structure through the remainder of the core. Macropores were observed throughout the mollic epipedon, while very fine tubular pores were observed throughout the B horizons. The cores reserved for micro-site properties were cut into 10 cm sections (0–10, 10–20, 20–30, 30–40, 40–50, 50–60, 60–70, and 70–80 cm) to follow natural horizonation in the soil core, while still aligning with the gas sampling depths. Core sections were analyzed for root length and mass, water-stable aggregate size distributions, and location of organic matter within the soil matrix (physical separation into available, aggregate-protected and mineral-bound C and N pools) as described below.

Cores were first analyzed for root properties on volumetric subsamples collected from the center of each core section with a 2.25 cm diameter probe. Visible litter was removed from each sub-sample and remaining soil + roots were immersed in deionized water overnight to moisten roots and slake aggregates attached to roots. Samples were gently washed with deionized water on nested 2000 and 250 μm sieves. Roots remaining on each sieve were transferred to trays and scanned for length using the WinRhizo program (Régent Instruments, Quebéc, QC). Roots were then dried at 55 °C and weighed to determine root mass on a weight per area basis within each depth.

Table 1
Soil profile description for an undisturbed Mollisol near Mandan, ND.

Depth (cm)	Horizon	Color	Structure	Pores
0–2	Oi			
2–5	A1	10YR 3/2	strong, fine and medium granular	macropores
5–16	A2	10YR 2/1	strong, medium and coarse granular	macropores
16–36	A3	10YR 2/1	moderate, medium and coarse granular	macropores
36–54	BA	10YR 3/2	weak, medium prismatic parting to moderate, fine and medium subangular blocks	common, very fine tubular pores
54–70	Bw1	10YR 4/2	moderate, medium prismatic parting to moderate, fine and medium angular blocky	common, very fine tubular pores
70+	Bw2	10YR 4/2	strong, coarse angular blocky	common, very fine tubular pores

Soils remaining after root samples were removed were dried at room temperature and gently sieved to 8000 μm. Identifiable roots and litter were removed from the samples using forceps. Water-stable aggregate size distributions (2000–8000 μm–large macroaggregates, 250–2000 μm–small macroaggregates, and 53–250 μm-microaggregates) were determined using a wet sieving protocol described by Six et al. (1998) and sand corrected according to Denef et al. (2001). Physical separation of organic matter into available, aggregate-protected and mineral-bound pools was conducted based on methods described by Six et al. (1998). The relationship between aggregate size classes and organic matter pool separation is conceptually diagramed in Fig. 1. Briefly, whole soil samples (10 g) were dried at 105 °C and suspended in 1.85 g cm^{-3} density sodium polytungstate (SPT). The samples were then placed under vacuum (138 kPa) and centrifuged for 60 min at 2500 rpm. Floating material (available pool; organic residues at various stages of decomposition held between aggregates; Stevenson and Cole, 1999) was aspirated through a 20 μm nylon filter, rinsed, dried at 55 °C, weighed and stored. Twelve 6 mm glass beads and 30 mL of 1.85 g cm^{-3} density SPT were added to the material remaining in the centrifuge tube (aggregate-protected pool, sand, silt and clay), shaken for 18 h and centrifuged for 60 min at 2500 rpm. Floating material (aggregate-protected pool; organic residues physically protected aggregates; Jastrow and Miller, 1998) was aspirated through a 20 μm nylon filter, rinsed, dried at 55 °C, weighed and stored. The remaining soil pellet (sand, silt and clay) was rinsed three times to remove SPT from the sample. The soil pellet was then sieved with a 53 μm sieve and glass beads removed to separate sand from silt and clay (mineral-bound pool; amorphous organic matter chemically bound to silt and clay particles; Christensen, 1996). All samples were dried at 55 °C, weighed and stored. Organic matter fractions were powder-ground to <53 μm and analyzed for C and N via dry combustion (Carlo Erba, Thermo Scientific, Waltham, MA, USA). Pool sizes were calculated using bulk density. Carbon:N ratios were used to indicate the potential for decomposition within each of these pools (with net mineralization generally occurring for C:N ratios < 20; Stevenson and Cole, 1999). Emissions of CO_2 and N_2O at 0 °C were normalized with depth per g of whole soil C for both gases, per g of available C for CO_2 and per g of aggregate-protected C for N_2O to indicate substrate-use efficiency with depth.

2.3. Statistical analyses

Differences among soil properties with depth were determined using one-way analysis of variance followed by a post-hoc multiple comparison of means (JMP 4.0.4, 2001). Level of significance was set at $P < 0.05$. A stepwise linear regression was used on micro-site property data (root mass, root length, aggregate size classes, available, aggregate-protected and mineral-bound C and N) to identify the properties that showed the greatest potential relationship (highest R^2) with CO_2 and N_2O emissions at 0 °C (α, Phillips et al., 2012). The gas sampling port at the surface (0 cm) was evaluated using soil data collected at the 0–10 cm soil depth, while the gas sampling port at subsequent intervals was evaluated using the soil depth increment immediately surrounding each port. Further, we tested if the soil property most strongly related to emissions of CO_2 and N_2O at 0 °C significantly affected the emissions at 0 °C using a mixed, random coefficients regression model (SAS 9.2, 2008).

3. Results

3.1. Soil structure and micro-site characteristics

Surface soils (<20 cm) contained a majority of the roots, as indicated by both mass and length (Fig. 2a and b). Trends in large

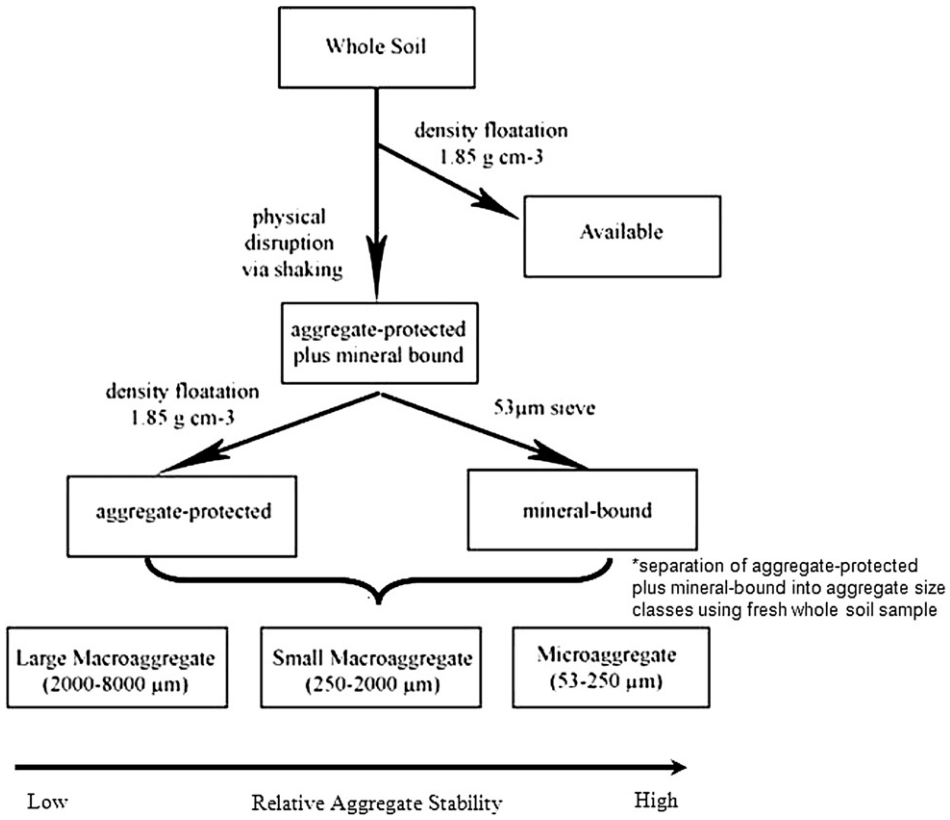

Fig. 1. Schematic diagram for the physical separation of whole soils into organic matter pools using high density fluid and aggregate fractions via wet sieving.

macroaggregate proportions with depth were similar to trends in root properties with depth. Large macroaggregate (2000–8000 μm) proportions decreased significantly within the surface 20 cm of soil (from 17 to 1% of total soil) and then were largely unchanged across all remaining depths (Fig. 2c). Between 30 and 45% of the soil was aggregated in the small macroaggregate size class (250–2000 μm), with similar proportions across all depths (0.39 ± 0.02 g aggregate g^{-1} soil; ±std error; data not shown). Microaggregates increased with depth throughout the mollic epipedon (approximately 0–40 cm) from 20 to 35% of total soil mass, and stayed consistent across subsoil depths (>40 cm; 0.35 ± 0.02 g aggregate g^{-1} soil; data not shown).

Whole soils were physically fractionated into available, aggregate-protected and mineral-bound C and N pools. The largest decrease in available C and N occurred within the surface soils (between the 0–10 and 10–20 cm depth; 2.8–1.3 Mg C ha^{-1} and 0.18–0.06 Mg N ha^{-1}), while at depths >20 cm C and N decreased much less, consistent with the root and large macroaggregate trends (Fig. 3a and b). Less than 10% of whole soil C and N was contained in the available soil fraction, with

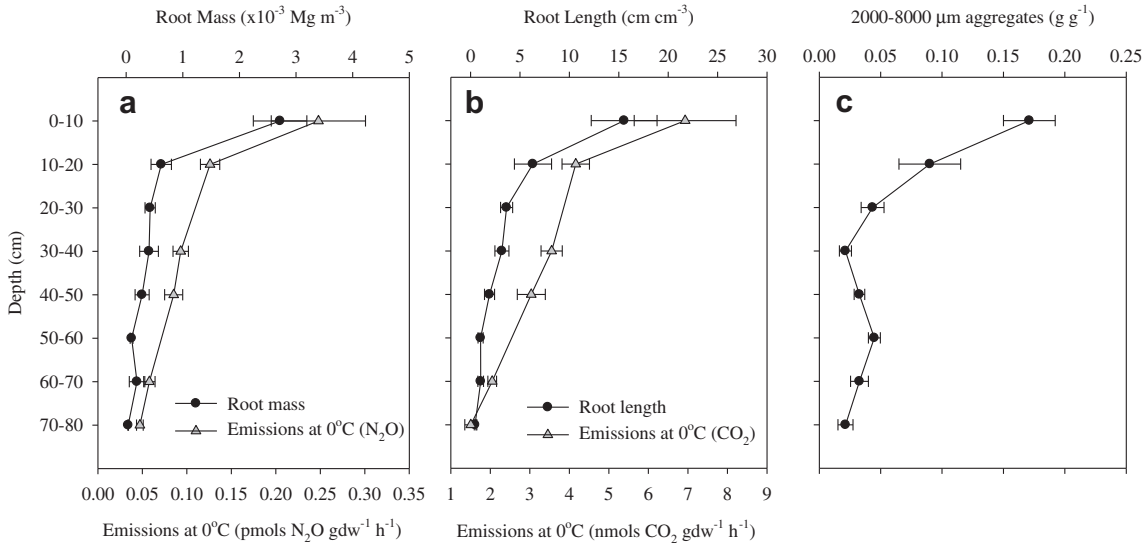

Fig. 2. (a) Root mass and emissions at 0 °C (N_2O), (b) root length and emissions at 0 °C (CO_2), and (c) large macroaggregate (2000–8000 μm) distribution with depth for an undisturbed Mollisol near Mandan, ND. Error bars represent standard error.

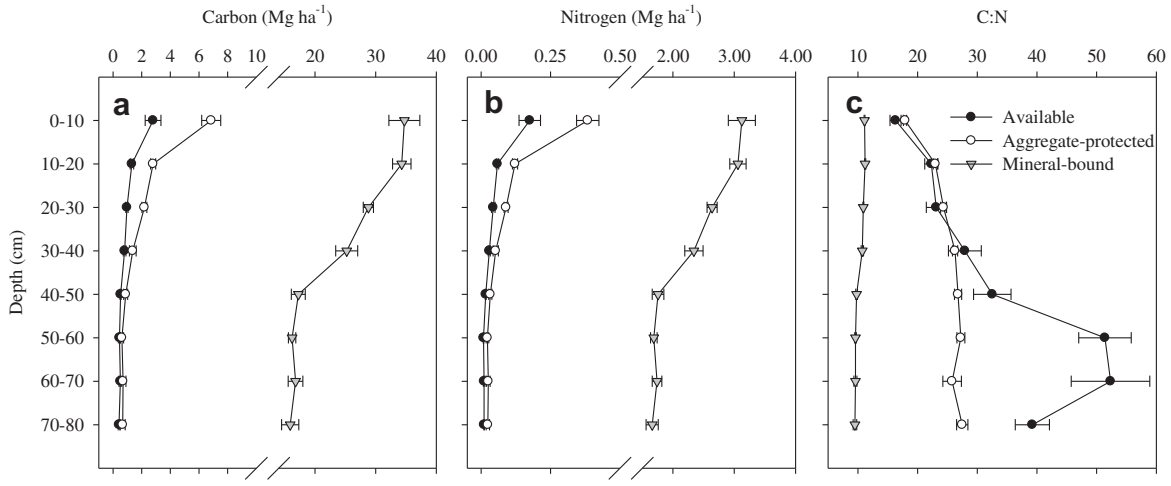

Fig. 3. (a) Carbon pools, (b) nitrogen pools, (c) C:N ratios for an undisturbed Mollisol near Mandan, ND. Soil pools determined using a physical fractionation technique, described by Six et al. (1998). Error bars represent standard error.

decreasing percentages with depth increments. Aggregate-protected C and N was consistently higher than available C and N across all depths and also declined more slowly with depth throughout the mollic epipedon than the available pool. Aggregate-protected C and N values decreased from 6.9 Mg C ha^{-1} and 0.38 Mg N ha^{-1} in the surface soils to 1.4 Mg C ha^{-1} and 0.05 Mg N ha^{-1} at the epipedon-subsoil contact. Values then remained similar throughout the subsoil. Mineral-bound C and N pool sizes were nearly five times that of the available and aggregate-protected C and N pool sizes, and again demonstrated a significant difference in values observed within the mollic epipedon versus the subsoil material. Mineral-bound C in the upper part of the mollic epipedon (0–20 cm depth) was 34.5 (±2.0) versus 27.0 (±1.6) Mg C ha^{-1} in the lower part of the epipedon (20–40 cm depths), while N averaged 3.1 (±0.20) Mg N ha^{-1} in the upper part of the epipedon and declined gradually to 2.3 Mg N ha^{-1} at the epipedon-subsoil contact. Mineral-bound pool sizes within the subsoil averaged 16.5 (±1.1) Mg C ha^{-1} and 1.7 (±0.09) Mg N ha^{-1}.

Available and aggregate-protected C:N gradually increased with depth, indicating the potentials for decomposition of both pools were lower in the subsoil than the mollic epipedon (Fig. 3c). Available C:N ratios averaged 22.4 (±2.5) in the mollic epipedon then increased significantly in the subsoil material (average 43.9 ± 5.6). Aggregate-protected C:N averaged 22.9 (±1.5) in the mollic epipedon and 26.8 (±0.98) in the subsoil. Mineral-bound organic matter in the epipedon had similar values, with 11.0 (±0.13) in the mollic epipedon and 9.6 (±0.22) in the subsoil.

3.2. Relationships between gas emissions at 0 °C and micro-site properties

Emissions at 0 °C (α) for both CO_2 and N_2O decreased exponentially with depth (Fig. 2a and b) and were strongly related to root length and root mass (Table 2). Large macroaggregate distribution trends also tracked emissions with depth (Fig. 2c). For CO_2, 7 out of 11 micro-site variables were significantly correlated ($R^2 > 0.56$) with α parameter estimates (Table 2). The highest coefficient of determination was for root length ($R^2 = 0.80$), followed by aggregate-protected C ($R^2 = 0.66$), available C ($R^2 = 0.65$), large macroaggregate mass ($R^2 = 0.63$), aggregate-protected N ($R^2 = 0.63$), and available N ($R^2 = 0.60$). For N_2O, 5 out of 11 micro-site variables were significantly related with α parameter estimates. The highest coefficient of determination was again for root length ($R^2 = 0.76$), followed by root mass ($R^2 = 0.74$), aggregate-protected C ($R^2 = 0.59$), aggregate-protected N ($R^2 = 0.57$), and large macroaggregate mass ($R^2 = 0.54$). Root length was most highly correlated with α for both gases, and the random coefficients model indicated root length significantly affected α for CO_2 ($F_{1,\ 4.56} = 41.96$; $p < 0.005$) and N_2O ($F_{1,\ 4.56} = 26.69$; $p < 0.005$).

Emissions of CO_2 and N_2O calculated on per g of whole soil C basis varied considerably from amounts calculated using per g of available or aggregate-protected C (Fig. 4a and b). Carbon dioxide emissions per g of whole soil C varied from 7.8 (±5.4) at the surface to 46.3 (±41.8) μmol CO_2–C g^{-1} whole C h^{-1} at the 75 cm depth (Fig. 4a), while CO_2 per g of available C ranged from 36.3 (±5.8) at the surface to 152.1 (±11.9) μmol CO_2–C g^{-1} available C h^{-1} at the 75 cm depth (Fig. 4b). Nitrous oxide emissions per g of whole soil C varied from 0.59 (±0.35) at the surface to 2.13 (±1.6) nmol N_2O–N g^{-1} whole C h^{-1} at the 75 cm depth (Fig. 4a), while N_2O per g of aggregate-protected C ranged from 1.53 (±0.28) at the surface to 11.0 (±4.5) nmol N_2O–N g^{-1} aggregate-protected C h^{-1} at the 75 cm depth (Fig. 4b). Differences between the mollic epipedon and subsoil were only observed when values were normalized by the individual soil C pools (available and aggregate-protected), indicating the importance of C pool selection when reporting gas fluxes per g of C.

Table 2
Relationships between CO_2 and N_2O emissions at 0 °C and soil micro-site variables for an undisturbed Mollisol (0–80 cm) near Mandan, ND determined using a step-wise linear regression. Bold indicates a significant relationship, symbol indicates level of significance.

Soil micro-site variable	R^2	
	CO_2	N_2O
Root length	**0.80****	**0.76****
Root mass	**0.56****	**0.74****
Large macroaggregate mass	**0.63****	**0.54****
Small macroaggregate mass	0.14	0.20
Microaggregate mass	0.41	0.46
Available C	**0.65***	0.44
Available N	**0.60***	0.39
Aggregate-protected C	**0.66****	**0.59****
Aggregate-protected N	**0.63****	**0.57***
Mineral-bound C	0.36	0.25
Mineral-bound N	0.35	0.24

*, ** indicate level of significance at $p \leq 0.05$ and 0.01, respectively.

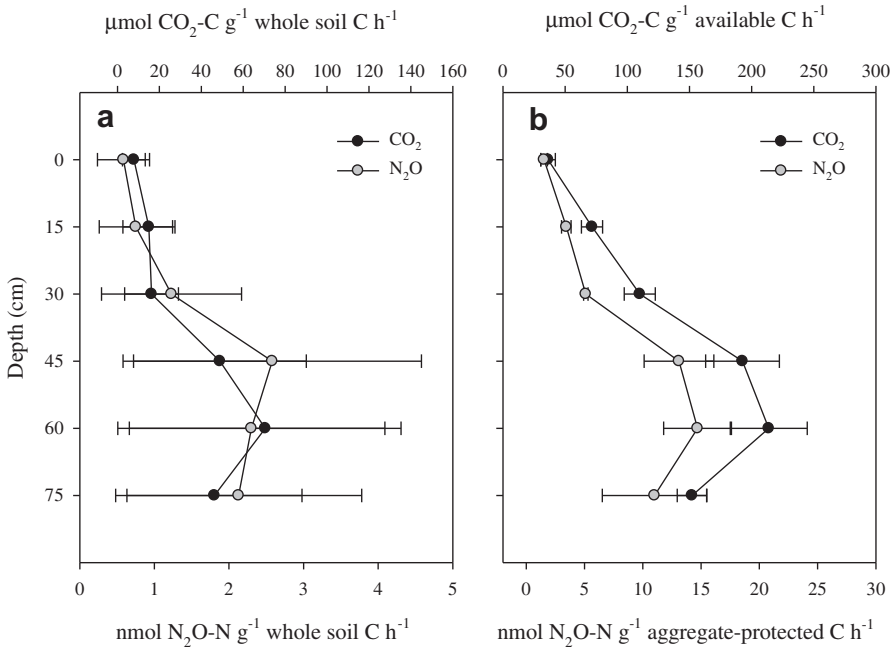

Fig. 4. (a) Normalized CO_2 and N_2O gas flux data by whole soil C, (b) normalized CO_2 and N_2O gas flux data by available and aggregate-protected pools, respectively, for an undisturbed Mollisol near Mandan, ND. Error bars represent standard error.

4. Discussion

Temperature exerts a strong influence on CO_2 and N_2O emissions during soil thawing (Phillips et al., 2012), but soil micro-site properties also influence CO_2 and N_2O emissions during thawing (van Bochove et al., 2000b; Fang et al., 2005; Knorr et al., 2005; Davidson and Janssens, 2006; Risk et al., 2008). Of the micro-site properties measured in this study, root length and mass, large macroaggregate mass and aggregate-protected C and N were correlated to both CO_2 and N_2O emissions at 0 °C, while available C and N were correlated with CO_2 emissions only. These results point to potential differences in substrate use for organisms producing CO_2 and N_2O belowground (Fierer et al., 2003b; Sey et al., 2008), where organic substrate held within aggregates (aggregate-protected) is inherently more complex than substrate held between aggregates (available pool; Jastrow and Miller, 1998; Stevenson and Cole, 1999).

Roots play an integral role in soil CO_2 and N_2O production by (1) providing inputs of labile organic substrate in the form of exudates and root detritus fueling microbial activity (Dormaar, 1990; Jastrow et al., 1998; Bird et al., 2011), (2) altering soil physical properties (i.e. porosity and pore size distribution) in the rhizosphere via wet–dry cycles and aggregate formation/stabilization (Jastrow and Miller, 1998; Dijkstra and Cheng, 2007) and (3) providing channels for the transfer of soil gases throughout the profile (Hillel, 1982). Root inputs and rhizosphere processes have been found to increase the rate of CO_2 production via decomposition (Bottner et al., 1999; Cheng and Kuzyakov, 2005; Fierer et al., 2005; Bird et al., 2011; Zhu and Cheng, 2011). Additionally, higher microbial biomass, diversity and activity is commonly observed in the rhizosphere relative to the subsoil (Fierer et al., 2003a), with bacteria utilizing substrates within immediate surroundings due to limited mobility in the soil (Jastrow et al., 2007). The limited mobility of bacteria is further amplified in frozen soils, where activity is restricted to unfrozen water films (Ostroumov and Siegert, 1996).

We found trends in root properties and large macroaggregates were similar with depth, which corroborates observations where roots were closely related to macroaggregate formation and stability (Jastrow et al., 1998). Both large macroaggregates and root properties were also highly correlated with CO_2 and N_2O emissions at 0 °C, which is likely attributed to their effects on the soil micro-environment. In a previous study by Jastrow et al. (1998), fine and very fine roots were identified as the most important factor in aggregate stabilization. Fine roots influence macroaggregation via localized physical entanglement, wetting and drying, exudate production and rhizodeposition to stimulate microbial activity, as well as continued contributions of organic material to the soil via root turnover (Jastrow et al., 1998). As a result of root penetration and organic matter additions, large macroaggregates protect the most recent inputs of organic matter (Elliott, 1986). They also contain an assemblage of macropores (diameter >10 μm), provide habitat for microbial communities, and create a network of soil pores facilitating the movement of dissolved organic and inorganic substances throughout the soil (Ranjard and Richaume, 2001). This assemblage of organic matter and abundance of macropores facilitates a more diverse environment for microbial activity than observed in smaller aggregate size classes (Oades and Waters, 1991). These factors can also lead to both abundant and variable microbial communities in relatively small spaces (Mummey et al., 2006). Substrate use by abundant, more diverse and potentially more efficient microbial communities in macroaggregates (Ranjard and Richaume, 2001) may explain relationships between large macroaggregates and CO_2 and N_2O emissions at 0 °C.

Available, aggregate-protected and mineral-bound C and N were all higher in the mollic epipedon (0–40 cm) versus subsoil (40–80 cm) depths for this specific soil by magnitudes of 3×, 5× and 2×, respectively. The relatively larger pool sizes of available and aggregate-protected organic matter in the mollic epipedon also have a higher potential for decomposition than the available and aggregate-protected pools in the subsoil material. This coincides with the higher CO_2 and N_2O emission rates observed in the mollic epipedon than the subsoil. The mineral-bound pool was not related to CO_2 or N_2O emissions despite the quantity and quality of organic matter observed in this pool. The mineral-bound pool is commonly

found to be the largest of the three pools (Davidson and Janssens, 2006; Plante et al., 2006) and is more decomposed and humified than organic material in the available and aggregate-protected fractions (Jastrow and Miller, 1998).

Using available and aggregate-protected C to normalize emissions of CO_2 and N_2O, respectively, we found that substrate-use efficiency increased with depth for both gasses. This may be due to the change in microbial biomass and community diversity with depth (Fierer et al., 2003b) as well as the stratification of organic substrate quantity and quality with depth (Paul and Clark, 1996). This was not observed when whole soil C values were used, indicating the importance of fractionating soil C pools for normalizing soil gas emission data. When roots and substrate are abundant, as in the mollic epipedon, utilization by microbial communities is less efficient than in the subsoil, where substrate is limited and microbial communities are more specialized (Fierer et al., 2003b).

In soils where temperatures fluctuate around 0 °C, soil aggregates tend to break apart and release once aggregate-protected organic material into the available organic matter pool (Sehy et al., 2004; Bronick and Lal, 2005). This may have occurred during this study to influence CO_2 and N_2O emission rates during thawing. The relationships observed among roots, large macroaggregates, organic matter stratification, and temperature are clearly important to the variability observed in CO_2 and N_2O emissions for these highly aggregated soils. Respiration rates reported in this study for multiple soil depths were greater than reports for arctic soil depths (Waldrop et al., 2010), but lower than soils found in warmer climates (Silver et al., 2005). Rates of CO_2 and N_2O emissions in frozen soils tend to be low and dominated by denitrification (Phillips, 2008; Sehy et al., 2004); nonetheless, emissions during thawing can represent a significant portion of the annual budget (van Bochove et al., 2000a). This study supports the assertion that substrate availability with respect to micro-site (rhizosphere and aggregate protection) is fundamental to microbial emissions of CO_2 and N_2O.

5. Conclusions

The magnitude of CO_2 and N_2O emissions at 0 °C were lower at deeper soil depths (>45 cm) and were highly related to micro-site properties, such as root length and mass, large macroaggregation, and available and aggregate-protected C and N. While CO_2 emissions were highly correlated with both available and aggregate-protected C and N, N_2O emissions were highly correlated with the less labile, aggregated-protected C and N. These relationships point to the importance of substrate pool or location when evaluating factors that influence CO_2 and N_2O emissions belowground and corroborate others that have suggested "hot spots" for N_2O production may be located within aggregate-protected micro-sites. We suggest future temperature-response investigations include multiple depth data on intact soils to better constrain those soil properties influencing emissions of CO_2 and N_2O. These results are specific to a historically native, northern prairie Mollisol, and additional investigations that include other soil series are needed.

Acknowledgments

The authors gratefully acknowledge support from Charles Walthall and Mark Walbridge from ARS National Program for Climate Change, Soils and Emission, Project number 5445-11120-002-00. We also thank Drs. Virginia Jin, Stephen Merrill and Catherine Stewart for their helpful comments during the preparation of this manuscript. We thank Joan Breiner (USDA-ARS), Becky Wald (USDA-ARS), Susanna Gomez (VT), Velva Groover (VT), and Julie Burger (VT) for field and lab assistance. We also appreciate the assistance of Dr. John Galbraith with soil classification and Dr. Roger Harris for assistance with root parameters. The mention of trade names, commercial products or organizations does not imply endorsement by the authors.

References

Ajwa, H.A., Rice, C.W., Sotomayor, D., 1998. Carbon and nitrogen mineralization in tallgrass prairie and agricultural soil profiles. Soil Science Society of America Journal 62, 942–951.
Bird, J.A., Herman, D.J., Firestone, M.K., 2011. Rhizosphere priming of soil organic matter by bacterial groups in a grassland soil. Soil Biology and Biochemistry 43, 718–725.
Bottner, P., Pansu, M., Sallih, Z., 1999. Modeling the effect of active roots on soil organic matter turnover. Plant and Soil 216, 15–25.
Bronick, C.J., Lal, R., 2005. Soil structure and management: a review. Geoderma 124, 3–22.
Burton, D.L., Beauchamp, E.G., 1994. Profile nitrous oxide and carbon dioxide concentrations in a soil subject to freezing. Soil Science Society of America Journal 58, 115–122.
Carter, M.R., 1996. Analysis of soil organic matter storage in agoecosystems. In: Carter, M.R., Stewart, B.A. (Eds.), Structure and Organic Matter Storage in Agricultural Soils. CRC Press, Inc., Boca Raton, FL, pp. 3–11.
Cheng, W.X., Kuzyakov, Y., 2005. Root effects on soil organic matter decomposition. Agronomy Monograph No. 48. In: Zobel, R.W., Wright, S.F. (Eds.), Roots and Soil Management: Interactions between Roots and the Soil. ASA-SSSA, Madison, Wisconsin.
Christensen, S., Christensen, B.T., 1991. Organic matter available for denitrification in different soil fractions: effect of freeze/thaw cycles and straw disposal. Journal of Soil Science 42, 637–647.
Christensen, B.T., 1996. Carbon in primary and secondary organomineral complexes. In: Carter, M.R., Stewart, B.A. (Eds.), Structure and Organic Matter Storage in Agricultural Soils. CRC Press, Inc., Boca Raton, FL, pp. 97–165.
Davidson, E.A., Janssens, I.A., 2006. Temperature sensitivity of soil carbon decomposition and feedbacks to climate change. Nature 440, 165–173.
Davidson, E.A., Savage, K.E., Trumbore, S.E., Borken, W., 2006. Vertical partitioning of CO_2 production within a temperate forest soil. Global Change Biology 12, 944–956.
del Prado, A., Merino, P., Estabillo, J.M., Pinto, M., Gonzalez-Murua, C., 2006. N_2O and NO emissions from different N sources under a range of soil water contents. Nutrient Cycling in Agroecosystems 74, 229–243.
Denef, K., Six, J., Bossuyt, H., Frey, S.D., Elliott, E.T., Merckx, R., Paustian, K., 2001. Influence of dry–wet cycles on the interrelationship between aggregate, particulate organic matter, and microbial community dynamics. Soil Biology and Biochemistry 33, 1599–1611.
Dijkstra, F.A., Cheng, W., 2007. Moisture modulates rhizosphere effects on C decomposition in two different soil types. Soil Biology and Biochemistry 39, 2264–2274.
Dormaar, J.F., 1990. Effects of active roots on the decomposition of soil organic materials. Biology and Fertility Soils 10, 121–126.
Elliott, E.T., 1986. Aggregate structure and carbon, nitrogen and phosphorous in native and cultivated soils. Soil Science Society of America Journal 50, 627–633.
Fang, C., Smith, P., Moncrieff, J.B., Smith, J.U., 2005. Similar response of labile and resistant soil organic matter pools to changes in temperature. Nature 433, 57–59.
Fierer, N., Allen, A.S., Schimel, J.P., Holden, P.A., 2003a. Controls on microbial CO_2 production: a comparison of surface and subsurface soil horizons. Global Change Biology 9, 1322–1332.
Fierer, N., Schimel, J.P., Holden, P.A., 2003b. Variations in microbial community composition through two soil depth profiles. Soil Biology and Biochemistry 35, 167–176.
Fierer, N., Chadwick, O.A., Trumbore, S.E., 2005. Production of CO_2 in soil profiles of a California annual grassland. Ecosystems 8, 412–429.
Gödde, M., Conrad, R., 1999. Immediate and adaptational temperature effects on nitric oxide production and nitrous oxide release from nitrification and denitrification in two soils. Biology and Fertility of Soils 30, 33–40.
Gregorich, E.G., Turchenek, L.W., Carter, M.R., Angers, D.A., 2001. Soil and Environmental Science Dictionary. CRC Press, Boca Raton, FL.
Henry, 2007. Soil freeze-thaw cycle experiments: trends, methodological weaknesses and suggested improvements. Soil Biology and Biochemistry 39, 977–986.
Hillel, D., 1982. Introduction to Soil Physics. Academic Press, San Diego, CA.
Jastrow, J.D., Miller, R.M., 1998. Soil aggregate stabilization and carbon sequestration. In: Lal, R., Kimble, J.M., Follett, R.F., Stewart, B.A. (Eds.), Soil Processes and the Carbon Cycle. CRC Press, Boca Raton, FL, pp. 207–233.
Jastrow, J.D., Miller, R.M., Lussenhop, J., 1998. Interactions of biological mechanisms contributing to soil aggregate stabilization in restored prairie. Soil Biology and Biochemistry 30, 905–916.
Jastrow, J.D., Amonette, J.E., Bailey, V.L., 2007. Mechanisms controlling soil carbon turnover and their potential application for enhancing carbon sequestration. Climatic Change 80, 5–23.
JMP 4.0.4., 2001. Division of SAS. SAS Institute, Cary, NC.

Jobbágy, E.G., Jackson, R.B., 2000. The vertical distribution of soil organic carbon and its relation to climate and vegetation. Ecological Applications 10, 423–436.
Killham, K., 1994. Soil Ecology. Cambridge University Press, Cambridge, UK.
Knorr, W., Prentice, I.C., House, J.I., Holland, E.A., 2005. Long-term sensitivity of soil carbon turnover to warming. Nature 433, 298–301.
Mikan, C.J., Schimel, J.P., Doyle, A.P., 2002. Temperature controls of microbial respiration in arctic tundra soils above and below freezing. Soil Biology and Biochemistry 34, 1785–1795.
Mummey, D., Holben, W., Six, J., Stahl, P., 2006. Spatial stratification of soil bacterial populations in aggregates of diverse soils. Microbial Ecology 51, 404–411.
Oades, J.M., Waters, A.G., 1991. Aggregate hierarchy in soils. Australian Journal of Soil Research 29, 815–828.
Ostroumov, V.E., Siegert, C., 1996. Exobiological aspects of mass transfer in microzones of permafrost deposits. Advances in Space Research 18, 79–86.
Parkin, T.B., 1987. Soil micro-sites as a source of denitrification variability. Soil Science Society of America Journal 51, 1194–1199.
Paul, E.A., Clark, F.E., 1996. Soil Microbiology and Biochemistry. Academic Press, San Diego, CA.
Phillips, R.L., 2008. Denitrification in cropping systems at sub-zero temperatures: a review. Agronomy for Sustainable Development, 87–93.
Phillips, R.L., Wick, A.F., Liebig, M.A., West, M., Daniels, W.L., 2012. Biogenic emissions of CO_2 and N_2O at multiple depths increase exponentially during a simulated soil thaw for a northern prairie Mollisol. Soil Biology and Biochemistry 45, 14–22.
Plante, A.F., Conant, R.T., Paul, E.A., Paustian, K., Six, J., 2006. Acid hydrolysis of easily dispersed and microaggregate-derived silt- and clay-sized fractions to isolate resistant soil organic matter. European Journal of Soil Science 57, 456–467.
Plante, A.F., Six, J., Paul, E.A., Conant, R.T., 2009. Does physical protection of soil organic matter attenuate temperature sensitivity? Soil Science Society of America Journal 73, 1168–1172.
Ranjard, L., Richaume, A., 2001. Quantitative and qualitative microscale distribution of bacteria in soil. Research in Microbiology 152, 707–716.
Risk, D., Kellman, L., Beltrami, H., Diochon, A., 2008. *In situ* incubations highlight the environmental constraints on soil organic carbon decomposition. Environmental Research Letters 3, 1–5.
SAS Version 9.2, 2008. SAS Institute Inc. USA, 205 Cary, NC.
Sehy, U., Dyckmans, J., Ruser, R., Munch, J., 2004. Adding dissolved organic carbon to simulate freeze-thaw related N_2O emissions from soil. Journal of Plant Nutrition and Soil Science 167, 471–478.
Sexstone, A.J., Parkin, T.B., Tiedje, T., 1988. Denitrification response to soil wetting in aggregated and unaggregated soil. Soil Biology and Biochemistry 20, 767–769.
Sey, B.K., Manceur, A.M., Whalen, J.K., Gregorich, E.G., Rochette, P., 2008. Small-scale heterogeneity in carbon dioxide, nitrous oxide and methane production from aggregates of a cultivated sandy-loam soil. Soil Biology and Biochemistry 40, 2468–2473.
Silver, W.L., Thompson, A.W., McGroddy, M.E., Varner, R.K., Dias, J.D., Silva, H., Crill, P.M., Kellers, M., 2005. Fine root dynamics and trace gas fluxes in two lowland tropical forest soils. Global Change Biology 11, 290–306.
Six, J., Elliott, E.T., Paustian, K., Doran, J.W., 1998. Aggregation and soil organic matter accumulation in cultivated and native grassland soils. Soil Science Society of America Journal 62, 1367–1376.
Soil Survey Staff, 2010. Keys to Soil Taxonomy. USDA-NRCS, 11th ed. U.S. Government Printing Office, Washington, DC.
Stevenson, F.J., Cole, M.A., 1999. Cycles of Soil, Carbon, Nitrogen, Phosphorous, Sulfur, Micronutrients. John Wiley and Sons, New York, NY.
van Bochove, E., Jones, H.G., Bertrand, N., Prévost, D., 2000a. Winter fluxes of greenhouse gases from snow-covered agricultural soil: intra-annual and interannual variations. Global Biogeochemical Cycles 14, 113–125.
van Bochove, E., Prévost, D., Pelletier, F., 2000b. Effects of freeze thaw and soil structure on nitrous oxide produced in a clay soil. Soil Science Society of America Journal 4, 138–143.
van't Hoff, J.H., 1898. Lectures on Theoretical and Physical Chemistry. Edward Arnold, London, UK.
Waldrop, M.P., Wickland, K.P., White Iii, R., Berhe, A.A., Harden, J.W., Romanovsky, V.E., 2010. Molecular investigations into a globally important carbon pool: permafrost-protected carbon in Alaskan soils. Global Change Biology 16, 2543–2554.
Zhu, B., Cheng, W., 2011. Rhizosphere priming effect increases the temperature sensitivity of soil organic matter decomposition. Global Change Biology 17, 2172–2183.